Journal of Solid State Chemistry 182 (2009) 2664–2669

Contents lists available at ScienceDirect

Journal of Solid State Chemistry

journal homepage: www.elsevier.com/locate/jssc

First-principles studies of Al–Ni intermetallic compounds

Dongmin Shi [a], Bin Wen [a,*], Roderick Melnik [b], Shan Yao [a], Tingju Li [a]

[a] School of Materials Science and Engineering, Dalian University of Technology, Dalian 116023, PR China
[b] M²NeT Lab, Wilfrid Laurier University, Waterloo, 75 University Ave. West, Ontario, Canada N2L 3C5

ARTICLE INFO

Article history:
Received 24 March 2009
Received in revised form
15 July 2009
Accepted 18 July 2009
Available online 24 July 2009

Keywords:
Nickel aluminides
Mechanical properties
Electrical properties
First-principle electron theory
Heats of formation
Multi-materials systems

ABSTRACT

The structural properties, heats of formation, elastic properties, and electronic structures of Al–Ni intermetallic compounds are analyzed here in detail by using density functional theory. Higher calculated absolute values of heats of formation indicate a very strong chemical interaction between Al and Ni for all Al–Ni intermetallic compounds. According to the computational single crystal elastic constants, all the Al–Ni intermetallic compounds considered here are mechanically stable. The polycrystalline elastic modulus and Poisson's ratio have been deduced by using Voigt, Reuss, and Hill (VRH) approximations, and the calculated ratio of shear modulus to bulk modulus indicated that AlNi, Al_3Ni, $AlNi_3$ and Al_3Ni_5 compounds are ductile materials, but Al_4Ni_3 and Al_3Ni_2 are brittle materials. With increasing Ni concentration, the bulk modulus of Al–Ni intermetallic compounds increases in a linear manner. The electronic energy band structures confirm that all Al–Ni intermetallic compounds are conductors.

1. Introduction

Due to potential technological applications as high-temperature materials, intermetallic compounds have attracted much attention in recent years. Among these intermetallic compounds, Al–Ni system compounds stand out as one of the most important and promising candidates for high-temperature materials for the use in harsh environments [1,2]. Furthermore, Al–Ni intermetallic compounds are emerging as important materials for nanotechnological applications with recent examples of applications of bimetallic Al–Ni reactive nanostructure as nanoheaters [3]. Al–Ni phase diagrams were first published by Gwyer in 1908 [4], and they have been re-examined experimentally and theoretically by many researchers since that time [5–18]. Based on these Al–Ni phase diagrams, it is known now that six intermetallic compounds can exist in an Al–Ni system compound, namely Al_3Ni, Al_3Ni_2, Al_4Ni_3, AlNi, Al_3Ni_5 and $AlNi_3$.

The properties of AlNi and $AlNi_3$ intermetallic compounds, owing to their important technological applications, have already been extensively investigated experimentally and theoretically. For example, various aspects such as the enthalpies of formation [19–23], equilibrium lattice constants, the elastic constants, the cohesive energy, and the effective defect formation energies have all been studied systematically [24]. As for the other Al–Ni intermetallic compounds, the studies of their properties have mainly focused on their heats of formation [7,10,25], and systematical studies on their other properties is still lacking in the literature. To fill this gap, in what follows the structural properties, heats of formation, elastic properties and electronic energy band structures of Al–Ni intermetallic compounds will be analyzed with first-principle methods.

2. Computational method

For our computational analysis of six Al–Ni intermetallic compounds (namely Al_3Ni, Al_3Ni_2, Al_4Ni_3, AlNi, Al_3Ni_5 and $AlNi_3$) we use density functional theory (DFT) and the plane-wave pseudopotential technique implemented in the CASTEP package [26]. The ion–electron interaction is modeled by ultrasoft pseudopotentials [27]. Generalized gradient approximation (GGA) [28] with the Perdew–Burke–Ernzerhof (PBE) [29] exchange-correlation functional is used. The kinetic cutoff energy for plane waves is set as 400 eV [30]. The **k** point separation in the Brillouin zone of the reciprocal space is 0.04 nm^{-1}, that is, $10\times10\times10$ for AlNi, $8\times8\times8$ for $AlNi_3$, $4\times3\times5$ for Al_3Ni, $7\times7\times6$ for Al_3Ni_2, $3\times4\times7$ for Al_3Ni_5, and $2\times2\times2$ for Al_4Ni_3, respectively.

Benchmark calculations have been conducted for the $AlNi_3$ phase, pointing out that the computational scheme utilized in this work is credible. Indeed, the calculated lattice parameter of 0.3561 nm compares well with the experimental value of 0.3566 nm [31]. We note also that the computed heat of formation for the $AlNi_3$ phase is −47.5 kJ/mol atoms, providing good agreement with experimental result of −47.3 kJ/mol atoms [32].

* Corresponding author. Fax: +86 411 8470 9284.
E-mail address: wenbin@dlut.edu.cn (B. Wen).

0022-4596/$ - see front matter © 2009 Elsevier Inc. All rights reserved.
doi:10.1016/j.jssc.2009.07.026

3. Results and discussion

3.1. Structural properties

First, by utilizing the experimental crystallographic data of the Al–Ni intermetallic compounds from Refs. [9,33–36] as the original configurations, the lattice parameters and internal coordinates of the Al–Ni intermetallic compounds have been optimized in this paper. The calculated values of lattice parameters and the corresponding mass densities, together with the experimental [31,35,37] and calculated [24,38–41] data are shown in Table 1. It can be seen from Table 1 that the lattice parameters and mass densities of Al–Ni intermetallic compounds are in good agreement with the experimental and other theoretical data, confirming that the proposed computational methodology is suitable for our current purpose and that the results from our geometry optimizations are reliable.

The relationship between mass densities and Ni concentration for different intermetallic compounds is shown in Fig. 1. As can be seen from Fig. 1, the computational mass densities increase with Ni concentrations in a linear manner. From a practical point of view, note that with increasing Ni concentration c (at%), the mass density ρ (kg/m^3) increases approximately with a linear relationship: $\rho = 2607.63+6365.90c$.

3.2. Elastic properties and mechanical stability

In this work, the elastic properties of the optimized crystal structures have already been obtained by using DFT calculations. Table 2 provides a summary of elastic constants C_{ij} (GPa) and bulk modulus of Al–Ni intermetallic compounds, together with the previous experimental and theoretical values [42–46].

To study the mechanical stability of Al–Ni intermetallic compounds, the elastic constants are investigated for all Al–Ni intermetallic compounds. The mechanical stability leads to restrictions on the elastic constants, which for cubic crystals are [47]

$$C_{11}>0, C_{44}>0, C_{11}-C_{12}>0, C_{11}+2C_{12}>0. \quad (1)$$

Table 1
Experimental and optimized crystallographic data and mass density of Al–Ni intermetallic compounds.

Compound	Space group	Mass density (kg/m^3)	Lattice parameters (nm)	Reference
Al	$Fm3m$	2710	$a = 0.4048$	This work
		2710	$a = 0.4047$	[39]
		2700	$a = 0.4050$	[37]
Al_3Ni	$Pnma$	4100	$a = 0.6565$, $b = 0.7257$, $c = 0.4750$	This work
		3930	$a = 0.6606$, $b = 0.7389$, $c = 0.4835$	[41]
		3980	$a = 0.6598$, $b = 0.7352$, $c = 0.4802$	[35]
Al_3Ni_2	$P\bar{3}m1$	4900	$a = b = 0.4002$, $c = 0.4848$	This work
Al_4Ni_3	$Ia\bar{3}d$	5220	$a = 1.1306$	This work
AlNi	$Pm\bar{3}m$	6040	$a = 0.2868$	This work
		5880	$a = 0.2895$	[40]
		5920	$a = 0.2886$	[31]
Al_3Ni_5	$Cmmm$	6730	$a = 0.7440$, $b = 0.6638$, $c = 0.3741$	This work
$AlNi_3$	$P4/mmm$	7500	$a = 0.3561$	This work
		7450	$a = 0.3565$	[40]
		7440	$a = 0.3566$	[28]
		7440	$a = 0.3566$	[27]
Ni	$Fm3m$	8870	$a = 0.3529$	This work
		8880	$a = 0.3528$	[39]
		8910	$a = 0.3524$	[37]

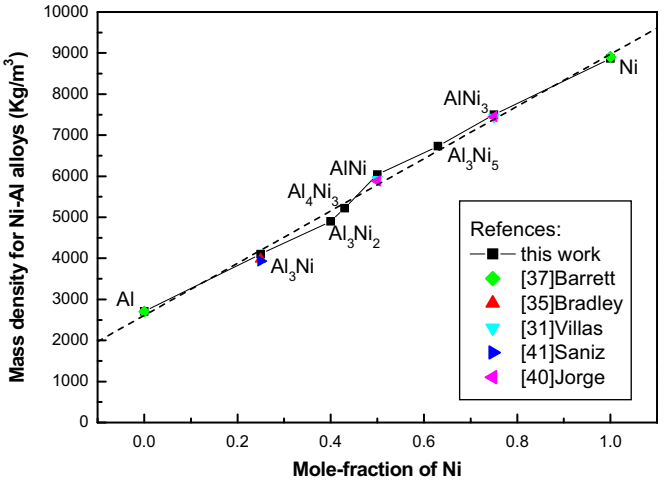

Fig. 1. Theoretical mass density compared to experimental values for the Al–Ni intermetallic compounds.

Table 2
Calculated elastic properties compared to experimental and other theoretical values for the single crystalline Al–Ni intermetallic compounds.

Compound	Elastic properties	Reference
Al_3Ni	$C_{11} = 169$, $C_{12} = 87$, $C_{13} = 94$, $C_{22} = 167$, $C_{23} = 81$, $C_{33} = 164$, $C_{44} = 89$, $C_{55} = 74$, $C_{66} = 51$, $K = 113$	This work
Al_3Ni_2	$C_{11} = 226$, $C_{12} = 57$, $C_{13} = 33$, $C_{33} = 317$, $C_{44} = 93$, $C_{66} = 85$, $K = 119$	This work
Al_4Ni_3	$C_{11} = 253$, $C_{12} = 68$, $C_{44} = 115$, $K = 129$	This work
AlNi	$C_{11} = 170$, $C_{12} = 158$, $C_{44} = 101$, $K = 162$	This work
	$K = 154$	[42] Ab initio
	$K = 156$	[43] Experimental
	$C_{11} = 183$, $C_{12} = 116$, $C_{44} = 93$	[24] EAM
	$C_{11} = 200$, $C_{12} = 140$, $C_{44} = 120$	[44] EAM
	$C_{11} = 199$, $C_{12} = 137$, $C_{44} = 116$, $K = 158$	[45] Experimental
	$C_{11} = 189$, $C_{12} = 131$, $C_{44} = 107$, $K = 150$	[46] PW
	$C_{11} = 199$, $C_{12} = 137$, $C_{44} = 116$, $K = 158$	[46] USPE
	$C_{11} = 197$, $C_{12} = 119$, $C_{44} = 110$, $K = 145$	[46] NS
Al_3Ni_5	$C_{11} = 234$, $C_{12} = 147$, $C_{13} = 93$, $C_{22} = 210$, $C_{23} = 144$, $C_{33} = 253$, $C_{44} = 109$, $C_{55} = 89$, $C_{66} = 126$, $K = 162$	This work
$AlNi_3$	$C_{11} = 229$, $C_{12} = 161$, $C_{44} = 125$, $K = 183$	This work
	$K = 182$	[42] Ab initio
	$C_{11} = 218$, $C_{12} = 120$, $C_{44} = 103$	[24] EAM

C_{ij}, elastic constants (GPa); K, bulk modulus (GPa); EAM, embedded atom method; PW, computed values; USPE, ultrasonic pulse-echo method; NS, slopes of measured acoustic phonon frequencies.

It can be seen from Table 2 that the elastic stiffness constants of the cubic structures (AlNi, $AlNi_3$ and Al_4Ni_3) satisfy the above restrictions in Eq. (1).

The mechanical stability criterion can be formulated in terms of the elastic constants for orthorhombic structures as [48]

$$C_{11}>0, C_{22}>0, C_{33}>0, C_{44}>0, C_{55}>0, C_{66}>0,$$
$$C_{11}+C_{22}-2C_{12}>0, C_{11}+C_{33}-2C_{13}>0, C_{22}+C_{33}-2C_{23}>0,$$
$$C_{11}+C_{22}+C_{33}+2C_{12}+2C_{13}+2C_{23}>0. \quad (2)$$

The elastic constants in the orthorhombic setting of Al_3Ni and Al_3Ni_5 fulfill all these stability criteria in Eq. (2).

There are three following restrictions for the mechanical stability of trigonal crystals [49]:

$$C_{11}-|C_{12}|>0, (C_{11}+C_{12})C_{33}-2C_{13}^2>0, (C_{11}-C_{12})C_{44}-2C_{14}^2>0. \quad (3)$$

All the values of elastic constants for trigonal Al_3Ni_2 obey these mechanical stability restrictions in Eq. (3).

According to above analysis, all the Al–Ni intermetallic compounds considered here are mechanically stable.

In order to better understand the mechanical properties of Al–Ni intermetallic compounds, bulk modulus (K), shear modulus (G), Young's modulus (E), and Poisson's modulus (v) for a polycrystalline material were deduced from single-crystal elastic stiffness constants by using Voigt, Reuss, and Hill (VRH) approximations [50], and these results together with the previous experimental and theoretical values are shown in Table 3. For AlNi compound, the calculated bulk modulus is slightly larger than the experimental value of 158 GPa [45], with a difference within 5%. For $AlNi_3$ alloy, the calculated Young's modulus is smaller than the experimental value of 210 GPa [51], with a difference within 7%. This difference may be attributed to the following reasons: first, defects in the materials were not considered in our calculations; second, the effects of anisotropy on the elastic properties were not taken into account in experimental measurements.

To interpret our results, we compare the calculated bulk modulus and the experimental and theoretical values for the Al–Ni intermetallic compounds by plotting them in Fig. 2. As can be seen, the results on the calculated bulk moduli show close to linear increases with the concentration of Ni. In particular, with increasing Ni concentration c (at%), the bulk modulus K (GPa) of Al–Ni intermetallic compounds increases approximately with a linear relationship: $K = 80+128c$.

Fig. 3 shows the Young's modulus E, and shear modulus G against the Ni concentration. According to Fig. 3, Al_4Ni_3 phase has the highest E and G values, whereas AlNi phase has lowest values. It is known that the hardness of materials is closely relevant to their Young's modulus, E, and shear modulus, G [52]. Although the relationship between hardness and the moduli are not identical, large values of the moduli represent high hardness for the materials. Therefore, the hardness of Al_4Ni_3 phase is the largest, while the AlNi phase is the smallest.

To study the brittleness and ductility properties of Al–Ni intermetallic compounds, ratio of shear modulus to bulk modulus, G/K, have also been calculated, and it can be seen as an empirical criterion of the extent of fracture range in materials [53]. From the computations, the G/K values are 0.49, 0.85, 0.81, 0.24, 0.46, and 0.40 for Al_3Ni, Al_3Ni_2, Al_4Ni_3, AlNi, Al_3Ni_5, and $AlNi_3$, respectively. Based on the G/K values, AlNi, Al_3Ni, $AlNi_3$ and Al_3Ni_5 compounds are considered as ductile materials, but Al_4Ni_3 and Al_3Ni_2 are brittle materials. This result can explain the experimental result of Gaydosh et al. [54]. In their literature, fine grain AlNi alloy exhibits ductility because of composition homogeneity by a rapid solidification processing. However, the bulk material of AlNi alloy is brittle at room temperature [1]. This disagreement may be due

Table 3
Polycrystalline bulk modulus, shear modulus, Young's modulus (GPa), Poisson's modulus for Al–Ni intermetallic compounds by using Voigt, Reuss, and Hill (VRH) approximations.

Compound	K_V	K_R	K_H	G_V	G_R	G_H	E	G/K	v
Al_3Ni	114	114	114	59	53	56	143	0.49	0.29
Al_3Ni_2	113	112	112.5	97	95	96	224	0.85	0.17
Al_4Ni_3	130	130	130	106	105	105.5	249	0.81	0.18
AlNi	162	162	162 158[a] 156[b] 154[c]	63	14	38.5	107	0.24	0.39
Al_3Ni_5	163	162	162.5	86	65	75.5	196	0.46	0.30
$AlNi_3$	184	184	184 182[c]	89	60	74.5	197 210[d]	0.40	0.32

K, bulk modulus (GPa); E, Young's modulus (GPa); v, Poisson's ratios.

[a] Ref. [45] Experimental.
[b] Ref. [43] Experimental.
[c] Ref. [42] Ab initio.
[d] Ref. [51] Experimental.

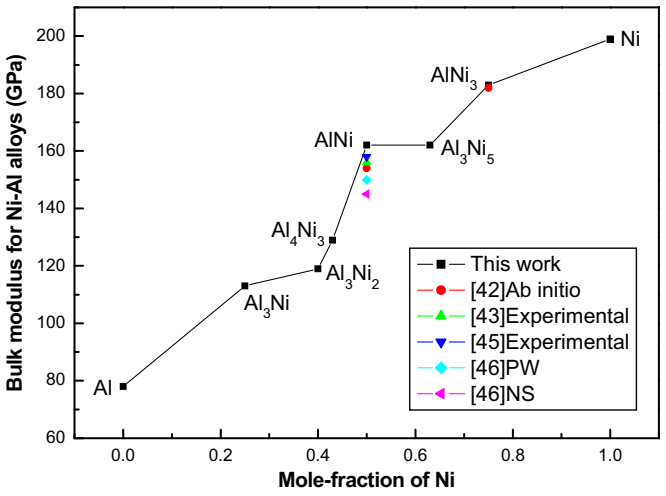

Fig. 2. Calculated bulk modulus compared to experimental and other theoretical values for the Al–Ni intermetallic compounds.

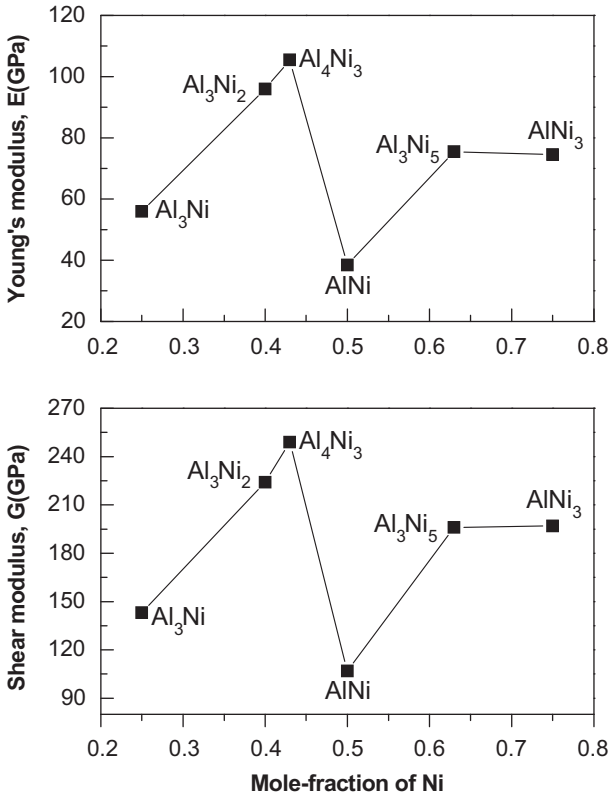

Fig. 3. Calculated shear modulus (G) and Young's modulus (E) versus concentration of Ni for the Al–Ni intermetallic compounds.

to the following reasons: first, the considered AlNi alloy is a pure substance, without accounting for the defects in the crystal; second, owing to the large difference of melting points for pure Ni (1726 K) and Al (933 K), AlNi alloy may have serious grain-boundary segregation under experimental conditions. The grain-boundary segregation leads to precipitation of Al-rich phases (Al_4Ni_3 and/or Al_3Ni_2) at grain-boundary, which brings about the brittleness of the alloy.

3.3. Thermodynamic stability and heat of formation

Through optimizing the 3D crystal structure of Al–Ni intermetallic compounds and the pure Ni and Al, we can obtain equilibrium crystal structures and ground state total energies for different Al–Ni intermetallic compounds. Then the heat of formation for Al–Ni intermetallic compounds can be calculated by the following formula:

$$E_{form}^{Al_mNi_n} = (E_{total}^{Al_mNi_n} - mE_{Al} - nE_{Ni})/(m+n) \quad (4)$$

where $E_{total}^{Al_mNi_n}$ refers to the total energy of an Al_mNi_n primitive cell that includes m Al atoms and n Ni atoms with equilibrium lattice parameters, E_{Al} is the total energy of an Al atom in the pure *fcc* Al metal with equilibrium lattice parameters, E_{Ni} is the total energy of a Ni atom in *fcc* Ni metal with equilibrium lattice parameters.

By using Eq. (4), the heats of formation have been calculated for all six intermetallic compounds. The calculated heats of formation of the Al–Ni intermetallic compounds are summarized in Table 4, along with the available experimental data and previous theoretical results [7,10,25,32,40,55–57]. Comparing the values, we found that our results are in very good agreement with these available experimental data and theoretical values. The result of this comparison is illustrated by Fig. 4. The graph exhibits a parabolic dependency and demonstrates that our results are in accordance with other values, confirming reliability of our computational methodology. Moreover, the absolute values of heats of formation for Al_3Ni, Al_3Ni_2, Al_4Ni_3, AlNi, Al_3Ni_5 and $AlNi_3$ are 42.1, 64.5, 65.9, 69.5, 61.5, and 47.5 kJ/mol atoms, indicating a very strong chemical interaction between Al and Ni because of higher values of heats of formation. All six intermetallic compounds are thermodynamically stable due to their negative heats of formation.

Table 4
The calculated and experimental heats of formation for Al–Ni intermetallic compounds.

Compound	Heat of formation (kJ/mol atoms)	Reference
Al_3Ni	−42.1	This work
	−22.2	[10] LMTO
	−37.7	[55] Experimental
Al_3Ni_2	−64.5	This work
	−75.2	[7] CALPHAD
	−62.7	[25] FLASTO
	−61.8	[10] LMTO
	−58.9	[57] Calorimetry
	−56.5	[55] Experimental
Al_4Ni_3	−65.9	This work
AlNi	−69.5	This work
	−66.8	[7] CALPHAD
	−73.3	[40] FLAPW
	−71.4	[56] LMTO
	−67.5	[32] Experimental
	−71.4	[57] Calorimetry
Al_3Ni_5	−61.5	This work
	−56.0	[25] FLASTO
$AlNi_3$	−47.5	This work
	−44.4	[25] FLASTO
	−48.2	[10] LMTO
	−47.3	[32] Experimental
	−45.7	[40] FLAPW
	−38.6	[57] Calorimetry

LMTO, linear muffin-tin orbital method; FLASTO, full-potential linearized augmented Slater-type orbital method; FLAPW, full potential linear augmented plane wave method; CALPHAD, calculation of phase diagrams.

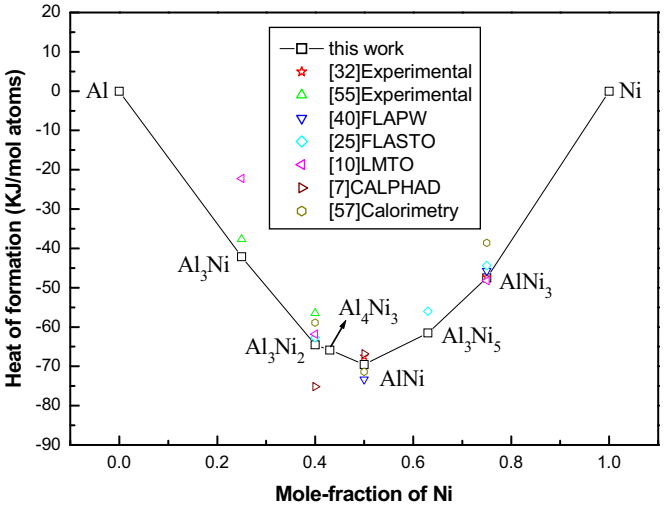

Fig. 4. Calculated heats of formation compared to experimental and other theoretical values for the Al–Ni intermetallic compounds.

3.4. Electronic energy band structure

Finally, the electronic energy band structures of the Al–Ni intermetallic compounds studied here with their optimized crystal lattices have also been calculated. The results are shown in Fig. 5. Electronic energy band structures indicate the energy of points which have symmetry in our intermetallic systems. The zero energy presented in the figure is the Fermi level which is defined as the highest occupied molecular orbital in the valence band at 0 K and located in the band gap. According to Fig. 5, the valence band overlaps the conduction band at the Fermi surface in the diagram of all six alloy compounds. Therefore, the Al–Ni intermetallic compounds we study are all conducting materials.

4. Conclusions

In summary, we have presented first-principles studies of the key properties of six Al–Ni binary intermetallic compounds (Al_3Ni, Al_3Ni_2, Al_4Ni_3, AlNi, Al_3Ni_5 and $AlNi_3$). The calculated lattice constants and heats of formation for Al–Ni intermetallic compounds are in good agreement with available experimental and previous theoretical values. With increasing Ni concentration, the mass density of Al–Ni intermetallic compounds increases in a linear manner. According to the computational single crystal elastic constants, all the Al–Ni intermetallic compounds considered here are mechanically stable. The polycrystalline elastic modulus and Poisson's ratio have been deduced by using Voigt, Reuss, and Hill (VRH) approximations, and the calculated ratio of shear modulus to bulk modulus indicated that AlNi, Al_3Ni, $AlNi_3$ and Al_3Ni_5 compounds are ductile materials, but Al_4Ni_3 and Al_3Ni_2 are brittle materials. With increasing Ni concentration, the bulk modulus of Al–Ni intermetallic compounds increases linearly. We have also provided the first-principles results on the heat

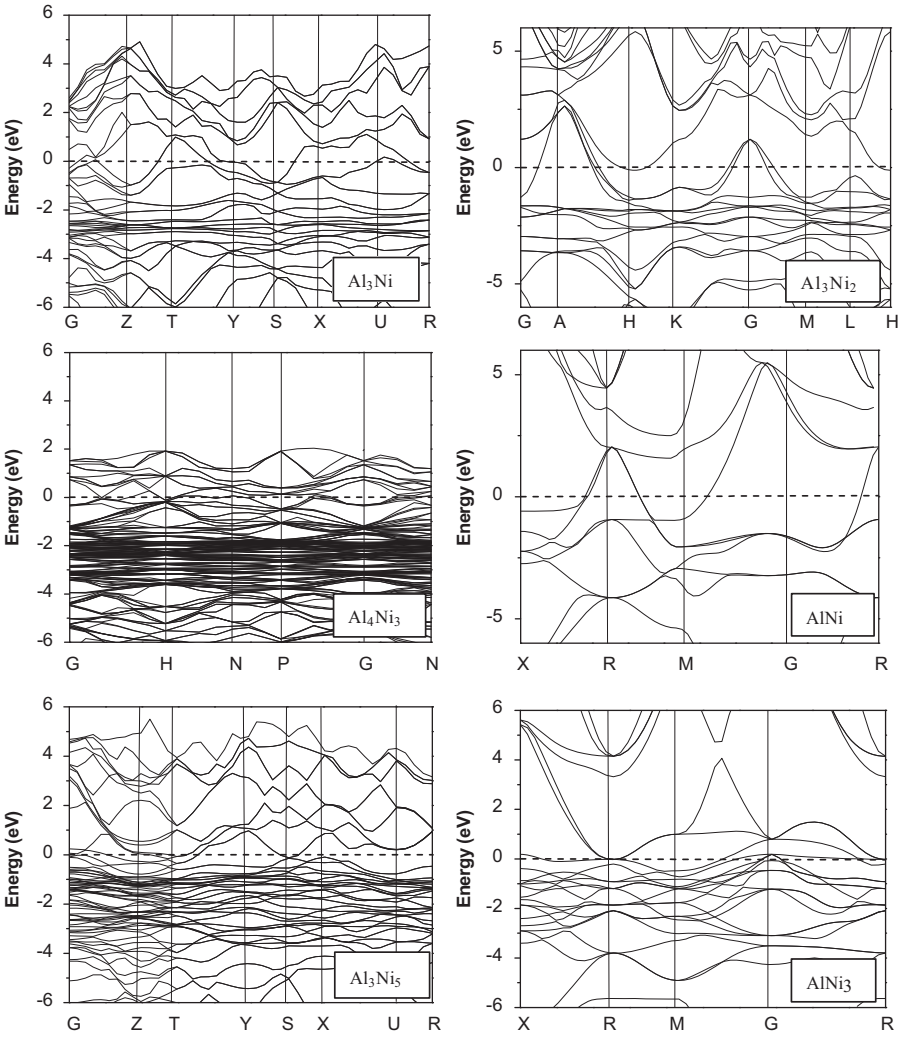

Fig. 5. Electronic energy band structures of Al–Ni intermetallic compounds.

of formations for the Al–Ni intermetallic compounds. In particular, the absolute values of heats of formation for Al_3Ni, Al_3Ni_2, Al_4Ni_3, AlNi, Al_3Ni_5 and $AlNi_3$ are 42.1, 64.5, 65.9, 69.5, 61.5, and 47.5 kJ/mol atoms, indicating a very strong chemical interaction between Al and Ni. Based on the calculation of the energy band structures we have concluded that all six Al–Ni intermetallic compounds studied here are conductors.

Acknowledgments

This work was supported by the National Natural Science Foundation of China (Grant nos. 50772018, 50402025) and the Program for New Century Excellent Talents in Universities of China (NCET-07-0139). R.M. acknowledges the support from the NSERC and CRC programs. B.W. acknowledges computational support from Prof. J.J. Zhao of Dalian University of Technology of China.

References

[1] C.T. Liu, Materials Chemistry and Physics 42 (1995) 77–86.
[2] B. Wen, J. Zhao, F. Bai, T. Li, Intermetallics 16 (2008) 333–339.
[3] H. Jogdand, G. Gulsoy, T. Ando, J. Chen, C.C. Doumanidis, Z. Gu, C. Rebholz, P. Wong, NSTI-Nanotech, vol. 1, 2008, ISBN 978-1-4200-8503-7, ⟨www.nsti.org⟩.
[4] A.G.C. Gwyer, Zeitschrift fur Anorganische und Allgemeine Chemie 57 (1908) 113.
[5] A.J. Bradley, A. Taylor, Proceedings of the Royal Society of London Series A 159 (1937) 56–72.
[6] L. Kaufman, H. Nesor, CALPHAD 2 (1978) 325.
[7] I. Ansara, B. Sundman, P. Willemin, Acta Metallurgica 36 (1988) 977–982.
[8] F.J. Bremer, M. Beyss, E. Karthaus, A. Hellwig, T. Schober, J.-M. Welter, H. Wenzl, Journal of Crystal Growth 87 (1988) 185–192.
[9] M. Ellner, S. Kek, B. Predel, Journal of the Less-Common Metals 154 (1989) 207–215.
[10] A. Pasturel, C. Colinet, A.T. Paxton, M. van Schilfgaarde, Journal of Physics: Condensed Matter 4 (1992) 945–959.
[11] H. Okamoto, Journal of Phase Equilibria 14 (1993) 257.
[12] P. Nash, M.F. Singleton, J.L. Murray, Phase Diagrams of Binary Nickel Alloys, ASM International, Materials Park, OH, 1991, pp. 3–11.
[13] P. Nash, Y.Y. Pan, Journal of Phase Equilibria 12 (1991) 105.
[14] K.J. Lee, P. Nash, Journal of Phase Equilibria 12 (1991) 551.
[15] Y. Du, N. Clavaguera, Journal of Alloys and Compounds 237 (1996) 20.
[16] I. Ansara, N. Dupin, H.L. Lukas, B. Sundman, Journal of Alloys and Compounds 247 (1997) 20–30.
[17] W. Huang, Y.A. Chang, Intermetallics 6 (1998) 487–498.
[18] F. Zhang, Y.A. Chang, Y. Du, S.-L. Chen, W.A. Oates, Acta Materialia 51 (2003) 207–216.
[19] K. Rzyman, Z. Moser, R.E. Watson, M. Weinert, Journal of Phase Equilibria 17 (1996) 173.
[20] K. Rzyman, Z. Moser, R.E. Watson, M. Weinert, Journal of Phase Equilibria 19 (1998) 106.
[21] K. Rzyman, Z. Moser, Progress in Materials Science 49 (2004) 581–606.
[22] R.X. Hu, P. Nash, Journal of Materials Science 40 (2005) 1067–1069.

[23] R. Arroyave, D. Shin, Z.K. Liu, Acta Materialia 53 (2005) 1809–1819.
[24] S. Yu, C.Y. Wang, T. Yu, J. Cai, Physica B: Condensed Matter 396 (2007) 138–144.
[25] R.E. Watson, M. Weinert, Physical Review B 58 (1998) 5981.
[26] M.D. Segall, P.J.D. Lindan, M.J. Probert, C.J. Pickard, P.J. Hasnip, S.J. Clark, M.C. Payne, Journal of Physics: Condensed Matter 14 (2002) 2717–2744.
[27] D.R. Hamann, M. Schluter, C. Chiang, Physical Review Letters 43 (1979) 1494.
[28] M.C. Payne, M.P. Teter, D.C. Allan, T.A. Arias, J.D. Joannopoulos, Reviews of Modern Physics 64 (1992) 1045.
[29] J.P. Perdew, K. Burke, M. Ernzerhof, Physical Review Letters 77 (1996) 3865.
[30] H.Y. Geng, N.X. Chen, M.H.F. Sluiter, Physical Review B 70 (2004) 094203.
[31] P. Villas, L. Calvert, Pearson's Handbook of Crystallographic Data for Intermetallic Phases, second ed., ASM International, Materials Park, OH, 1991.
[32] V.M. Es'kov, V.V. Samokhval, A.A. Vecher, Russian Metallurgy 2 (1974) 118.
[33] Y.I. Dutchak, V.G. Chekh, Russian Journal of Physical Chemistry 55 (1981) 1326–1328 Translated from Zhurnal Fizicheskoi Khimii.
[34] P.V. Mohan Rao, K. Satyanarayana Murthy, S.V. Suryanarayana, S.V. Nagender Naidu, Physica Status Solidi Section A: Applied Research (1992) 231–235.
[35] A.J. Bradley, A. Taylor, Philosophical Magazine 23 (1937) 1049–1067.
[36] K. Enami, S. Nenno, Transactions of the Japan Institute of Metals 19 (1978) 571–580.
[37] C.S. Barrett, T.B. Massalski, in: Structure of Metals, third ed., Pergamon Press, Oxford, 1980.
[38] G. Ghosh, G.B. Olson, Acta Materialia 55 (2007) 3281–3303.
[39] E.G. Moroni, G. Kresse, J. Hafner, J. Furthmuller, Physical Review B 56 (1997) 15629.
[40] J.E. Garcés, G. Bozzolo, Physical Review B 71 (2005) 134201.
[41] R. Saniz, Y.E. Lin-Hui, T. Shishidou, A.J. Freeman, Physical Review B 74 (2006) 014209.
[42] Y. Wang, Z.K. Liu, L.Q. Chen, Acta Materialia 52 (2004) 2665–2671.
[43] J.W. Otto, J.K. Vassiliou, G. Frommeyer, Journal of Materials Research 12 (1997) 3106–3108.
[44] Y. Mishin, M.J. Mehl, D.A. Papaconstantopoulos, Physical Review B 65 (2002) 224114.
[45] N. Rusovic, H. Warlimont, Physica Status Solidi A 44 (1977) 609.
[46] X.Y. Huang, I.I. Naumov, K.M. Rabe, Physical Review B 70 (2004) 064301.
[47] J.F. Nye, in: Physical Properties of Crystals, Oxford University Press, Oxford, 1985.
[48] O. Beckstein, J.E. Klepeis, G.L.W. Hart, O. Pankratov, Physical Review B 63 (2001) 134112.
[49] T. Tsuchiya, T. Yamanaka, M. Matsui, Physics and Chemistry of Minerals 27 (2000) 149–155.
[50] O.L. Anderson, The Journal of Physics and Chemistry of Solids 24 (1963) 909.
[51] T. Goto, T. Sasaki, Y. Hirose, JCPDS—International Centre for Diffraction Data (1999) 518.
[52] J. Haines, J.M. Léger, G. Bocquillon, Annual Review of Materials Research 31 (2001) 1.
[53] S.F. Pugh, The Philosophical Magazine 45 (1954) 823.
[54] D.J. Gaydosh, R.W. Jech, R.H. Titran, Journal of Materials Science Letters 4 (1985) 138–140.
[55] R. Hultgren, P.D. Desai, D.T. Hawkins, M. Gleiser, K.K. Kelley, Select Values of the Thermodynamic Properties of Binary Alloys, American Society for Metals, Metals Park, OH, 1973, p. 192.
[56] W. Lin, A.J. Freeman, Physical Review B 45 (1992) 61.
[57] P.D. Desai, Journal of Physical and Chemical Reference Data 16 (1987) 109.